Published in final edited form as:
J Am Water Resour Assoc. 2023 March 25; 59(4): 726–742. doi:10.1111/1752-1688.13109.

Modeling future land cover and water quality change in Minneapolis, MN, USA to support drinking water source protection decisions

Sean A. Woznicki[1], **George Kraynick**[2], **James Wickham**[1], **Maliha Nash**[3], **Terry Sohl**[4]

[1]Center for Public Health and Assessment, Office of Research and Development, United States Environmental Protection Agency, Research Triangle Park, North Carolina, USA

[2]City of Minneapolis Department of Public Works, Division of Water Treatment and Distribution Services, Minneapolis, Minnesota, USA

[3]Center for Public Health and Assessment, Office of Research and Development, United States Environmental Protection Agency, Newport, Oregon, USA

[4]Earth Resources Observation and Science Center, United States Geological Survey, Sioux Falls, South Dakota, USA

Abstract

Continued alteration of the nitrogen cycle exposes receiving waters to elevated nitrogen concentrations and forces drinking water treatment services to plan for such increases in the future. We developed four 2011–2050 land cover change scenarios and modeled the impact of projected land cover change on influent water quality to support long-term planning for the Minneapolis Water Treatment Distribution Service (MWTDS) using Soil Water and Assessment Tool. Projected land cover changes based on relatively unconstrained economic growth led to substantial increases in total nitrogen (TN) loads and modest increases in total phosphorus (TP) loads in spring. Changes in sediment, TN, and TP under two "constrained" growth scenarios were near zero or declined modestly. Longitudinal analysis suggested that the extant vegetation along the Mississippi River corridor upstream of the MWTDS may be a sediment (and phosphorus) trap. Autoregressive analysis of current (2008–2017) chemical treatment application rates (mass

Correspondence Sean A. Woznicki, Center for Public Health and Assessment, Office of Research and Development, United States Environmental Protection Agency, Research Triangle Park, NC, USA, woznicse@gvsu.edu.
Present address Sean A. Woznicki, Annis Water Resources Institute, Grand Valley State University, Muskegon, Michigan, USA

AUTHOR CONTRIBUTIONS

Sean A. Woznicki: Conceptualization; formal analysis; methodology; visualization; writing – original draft; writing – review and editing. **George Kraynick:** Investigation; methodology. **James Wickham:** Conceptualization; formal analysis; investigation; methodology; visualization; writing – original draft; writing – review and editing. **Maliha Nash:** Formal analysis; methodology. **Terry Sohl:** Data curation; methodology; writing – review and editing.

CONFLICT OF INTEREST STATEMENT

The authors have no conflicts of interest to disclose.

SUPPORTING INFORMATION

Additional supporting information can be found online in the Supporting Information section at the end of this article.

per water volume processed) and extant (2001–2011) land cover change revealed that statistically significant increases in chemical treatment rates were temporally congruent with urbanization and conversion of pasture to cropland. Using the current trend in chemical treatment application rates and their inferred relationship to extant land cover change as a bellwether, the unconstrained growth scenarios suggest that future land cover may present challenges to the production of potable water for MWTDS.

Keywords

drinking water; land cover change; SWAT; FORE-SCE; source water protection

1 | INTRODUCTION

The benefits of source water protection were recognized in the United States (U.S.) Safe Drinking Water Act Amendments of 1996 (P.L. 104–182) (Tiemann, 2017; Wickham et al., 2011). Natural landscapes (e.g., forests) protect drinking water sources by minimizing sediment erosion and other nonpoint source pollution, thereby maintaining the quality of raw water that will eventually be treated and distributed for consumption (McDonald et al., 2016). Postel and Thompson (2005) highlighted seven cities in the U.S. that have avoided expenditure of millions of dollars in capital and operational costs through protection of their source water. Warziniack et al. (2017) found that source water turbidity increases as forest cover declined and that treatment costs increased as turbidity increased. Fiquepron et al. (2013), Elias et al. (2014), and Heberling et al. (2015) have further advanced the research by developing quantitative relationships between drinking water treatment costs and watershed condition.

The benefits of source water protection are clear, but watershed condition continues to decline globally due to population growth, urbanization, and agricultural expansion. Since 1900, 90% of the largest cities (>750,000 population) in the world experienced degradation of their source watersheds, and 29% of these cities had a significant increase in their water treatment costs due to that degradation (McDonald et al., 2016). Threats to source water are apparent in the U.S., including urbanization, agricultural expansion, and the loss of natural lands. Population in the U.S. is projected to increase by 98.1 million between 2014 and 2060 (Colby & Ortman, 2017). Urban expansion is a threat to protected areas in the U.S., potentially displacing natural vegetation (Martinuzzi et al., 2015), and cropland area increased by 3 million acres between 2008 and 2012 in the U.S. (Lark et al., 2015).

Minnesota has experienced loss of natural lands to both agriculture and urbanization. Multiple studies have documented conversion of natural grassland to agriculture in Minnesota during 2008–2013 (Lark et al., 2019; Mladenoff et al., 2016). Minnesota's population grew by 6.1% from 2010 to 2018 (MN State Demographic Center, 2019a), with the largest growth occurring in the Minneapolis metropolitan region. By 2050, Minnesota's population is projected to increase from 5.62 million people to 6.37 million people (MN State Demographic Center, 2019b). These stressors are expected to impact surface water quality and drinking water in Minneapolis, which withdraws water from the Mississippi

River. The forests in the city's source water watershed are important for protecting drinking water (Weidner & Todd, 2011).

Considering these ongoing and future threats to drinking water quality, the objective of this study was to develop projections of land cover change and associated impacts of change on water quality constituents relevant to Minneapolis' drinking water treatment process. We use Soil Water and Assessment Tool (SWAT) to model the effects of projected land cover change for the year 2050. Modeling the effect of future land cover on source water quality is also supported by autoregressive (AR) models of recent trends in the application of drinking water treatment chemicals and the effect of recent land cover change (2001–2011) on water quality.

2 | METHODS

2.1 | Study area

The study watershed is the Mississippi Headwaters (MHW), 4-digit hydrologic unit code (HUC-4) 0701, in Minnesota with the outlet defined just south of the Minneapolis, MN drinking water intake. The land cover composition (Figure 1) of the 50,335 km^2 MHW watershed is primarily agriculture (33%), forest (27%), and wetlands (24%). Surface water (lakes and rivers) and urban land cover about 8% and 6% of the MHW, respectively. Dominant crops are corn and soybeans. Pastureland is about 29% of the land devoted to agriculture (10% of the watershed). There is a strong north–south gradient in the distribution of land cover, with the north dominated by forest, wetland, and surface water, and the south dominated by agriculture. The Minneapolis-St. Paul metropolitan area and other urban centers are in the southeastern section of the watershed. The southeastern parts of the watershed receive more precipitation than the northwest. Annual average precipitation from 1981 to 2010 for Minneapolis-St. Paul is 777 mm, whereas northwestern parts of the watershed average 676 mm annually.

The Minneapolis Water Treatment Distribution Service (MWTDS) withdraws water from the Mississippi River as its sole source, pumping about 21 billion gallons per year (79.5 million m^3/year) and providing drinking water for over 500,000 people. Multiple treatment processes are used, including softening, sedimentation, filtration (both granular activated carbon and membrane ultrafiltration), and disinfection. About 100 km upstream from Minneapolis, St. Cloud, MN produces potable water for over 68,000 people. Raw water from the Mississippi River is treated using a three-stage system, where it is treated with powder activated carbon (PAC) and alum (stage 1), followed by treatment with lime and CO_2 (stage 2), and then sent to a detention basin where it is filtered and disinfected (stage 3). A substantial upgrade of the St. Cloud water treatment facility is ongoing.

2.2 | Watershed model

Soil Water and Assessment Tool (Arnold et al., 1998) is a semi-distributed, process-based watershed model that examines the impacts of land management practices on watershed hydrology and water quality at various spatial scales. Major routines within SWAT include landscape runoff and water balance, erosion, river routing, nutrient cycling, crop growth, and

land management operations. In SWAT, the watershed is delineated into subbasins, which are further partitioned into hydrologic response units (HRUs). HRUs are nonspatial units of uniform land cover, soil type, slope class, and agricultural practices within each subbasin. The Modified Universal Soil Loss Equation is used to estimate sediment yield from the HRU. Transport and transformation of multiple forms of nitrogen and phosphorus are simulated in their respective cycles, with in-stream transport occurring via forms adsorbed to sediment or dissolved in water (Neitsch et al., 2011).

SWAT2012 (revision 670; Arnold et al., 2012) was used for simulation. The primary spatial and temporal inputs for parameterization were as follows: the one arc-second digital elevation model from the U.S. Geological Survey (USGS) 3D Elevation Program, the 30 m National Land Cover Database (NLCD) (Homer et al., 2015), which includes land cover for 2001, 2006, and 2011, the State Soil Geographic Database (STATSGO2) at 1:250,000 resolution, and gridded daily precipitation, minimum temperature, and maximum temperature from PRISM at 4 km resolution (PRISM Climate Group, Oregon State University, http://prism.oregonstate.edu). Secondary datasets and sources used to parameterize the SWAT model are listed in Table A1 (Supporting Information). The MHW was delineated into 815 subbasins and 14,160 HRUs.

The NLCD 2006 was used for calibration and uncertainty analysis because it was temporally central to available water quality data for SWAT calibration. Corn–soybean crop rotations were implemented on NLCD cropland. The most common crop rotations in the watershed were corn following corn and corn following soybeans (Bierman et al., 2012). Planting and harvest dates were defined using the U.S. Department of Agriculture (USDA) Field Crops Usual Planting and Harvesting Dates guide (USDA, 2010).

Calibration, validation, and uncertainty analysis were performed using the Sequential Uncertainty Fitting (SUFI-2) algorithm within SWAT-CUP v5.1.6.2 (SWAT Calibration and Uncertainty Programs) (Abbaspour, 2007). SUFI-2 expresses parameter uncertainty as uniform distributions, where the uncertainty is propagated to the model outputs, expressed as 95% probability distributions or 95% prediction uncertainty (95PPU). Nash Sutcliffe Efficiency greater than 0.5 (Moriasi et al., 2007) was used as the objective function for 95PPU behavioral simulations. To quantify the model fit between observations and the 95PPU, P-factor (percentage of observations enveloped by 95PPU) and R-factor (mean 95PPU thickness divided by standard deviation of observations) were used. P-factor >0.7 and R-factor <1.5 were desirable (Abbaspour et al., 2015).

Six USGS stream gages were used for discharge calibration/uncertainty analysis and six co-located Minnesota Pollution Control Agency (MPCA) water quality sampling locations (Figure 1) were used for calibration/uncertainty analysis of sediment load, total nitrogen (TN) load, and total phosphorus (TP) load.

The USGS Load Estimator (LOADEST) (Runkel et al., 2004) was used to estimate monthly constituent loads for the water quality sampling locations based on regression equations of grab sample concentrations as a function of daily discharge and date. LOADEST outputs (Tables A2-A4 in the Supporting Information) had low positive bias in the load estimation

of sediment (<10% percent bias) and negligible bias in TN and TP estimation (<2%) for any given water quality sampling and discharge location pair.

The simulation time period was 2001–2012, which included all available water quality data. Measurement uncertainty was included in SWAT-CUP for discharge, sediment, TN, and TP based on average values from Harmel et al. (2006). Results of combined calibration, validation, and uncertainty analysis are presented in Table A5 (Supporting Information) for all locations.

2.3 | Land cover change model

The FOREcasting Scenarios of Land-use Change (FORE-SCE) modeling framework developed by the USGS (Sohl et al., 2007) was used to create land cover scenario projections for 2050. FORE-SCE consists of annual land cover projections to 2100 for the continental U.S. at a 250-m resolution, based on scenarios developed for the Intergovernmental Panel on Climate Change (IPCC) Special Report on Emission Scenarios (SRES) (Nakicenovic et al., 2000).

We downscaled four SRES scenarios rendered at 250-m pixel resolution (Sohl et al., 2014) to a 30-m pixel resolution: A1B, A2, B1, and B2 (Supporting Information). The first letters (A, B) in the scenarios denote a dichotomy between material wealth (A) and sustainability and equity (B) and the numerals (1, 2) denote a dichotomy between globalization (1) and regionalization (2) of economic drivers and social policy (Strengers et al., 2004). Summaries of the four scenarios are as follows: a consumption-oriented population operates in a world where socioeconomic forces operate globally (A1); local constraints focused on sustainability constrain global socioeconomic forces (B1); a consumption-oriented population operates in a world where socioeconomic forces vary regionally (A2); and a population focused on sustainable use operates in a world where socioeconomic forces vary regionally (B2). The A1 group has three outcomes (scenarios), whereas the other three groups have only one outcome. A1B is a “balanced” scenario intermediate between a fossil fuel intensive (A1FI) scenario and a non-fossil fuel dominated (A1T) scenario (Nakicenovic et al., 2000). Agricultural trade is a useful example to distinguish between globally and regionally predominant socioeconomic forces. The amount of agricultural land in the U.S. might increase under the scenarios where socioeconomic forces are globally predominant to satisfy demand elsewhere, whereas an increase in the amount of area devoted to agriculture might be less when socioeconomic forces vary regionally. Sustainability denotes world views that emphasize efficient use of fertilizers or public transportation, whereas a consumption-oriented world view would not. Each scenario exhibits different land cover characteristics when the narratives are translated. These global characteristics (Strengers et al., 2004) were modified by Sohl et al. (2014) to better fit the conditions and characteristics of the conterminous U.S.

The downscaling techniques used were consistent with recommendations for localizing the global IPCC scenarios (Sleeter et al., 2012; van Vuuren et al., 2007, 2010). We created 2010–2050 land cover change matrices for the four scenarios (hereafter, scenario database). The land cover change matrices were used to derive a target estimate of the area of change for each land cover transition (e.g., deciduous forest to urban). Land cover changes were

restricted to the classes in scenario database that also occurred in NLCD 2011. We did not include changes in the scenario database classes “Disturbed National Forest,” “Disturbed, other,” “Disturbed, private,” and “Mining” because these classes were not mapped in NLCD 2011. We also did not include changes in “Barren,” “Grassland,” and “Shrubland.” These classes occurred in NLCD 2011 and the scenario database, but they were essentially nonexistent in the scenario database for the MHW. After determining the area of each change class, we overlaid the changes on a map of NLCD 2011 land cover patches, where a patch was defined as contiguous (8-neighbor) pixels of the same land cover class. NLCD 2011 patches that included a change pixel with the same land cover labels for NLCD 2011 and the 2010 scenario database served as the set of NLCD land cover patches that could transition from a 2010 land cover class to a 2050 land cover class. Random selection of NLCD 2011 patches was used when the total area of land cover patches that could change exceeded the target estimate for that change class. In some cases, the total area of NLCD 2011 patches was less than the estimated area of change in the scenario database. This issue tended to arise when the NLCD 2011 land cover classes evergreen forest, mixed forest, woody wetland, or emergent wetland changed to urban, cropland, or pasture in 2050. We increased the total amount of deciduous forest loss between 2010 and 2050 when this occurred. There was only a single class for urban in the FORE-SCE scenarios and therefore our downscaled scenarios did not identify change to the four, more detailed urban classes in NLCD. Because of the lack of urban specificity in the FORE-SCE models, our 2010 scenarios included the four NLCD urban classes and our 2050 scenarios included the same four NLCD urban classes plus a generalized urban land cover representing urbanization between 2010 and 2050.

Because of the random selection of patches for 2010–2050 land cover change, the resulting per-scenario spatial pattern was just one rendition of perhaps an infinite number of spatial patterns of change that could be realized from repeated implementation of the change model. The resulting spatial pattern likely influences SWAT results and is a source of uncertainty in the model. For example, if forest loss was heavily concentrated north of St. Cloud (gage 05270700 in Figure 1), the effects of forest loss on water quality at the MWTDS may be different than if forest loss was concentrated in and around the Minneapolis-St. Cloud corridor.

We implemented two versions of each scenario. One implementation allowed cropland and pasture to revert to forest, labeled with an f (e.g., A1Bf). The other version did not allow agriculture to revert to forest (e.g., A1B). We implemented the version that excluded 2010–2050 conversions of agriculture to forest to highlight the benefits of natural succession, conservation, and restoration in the context of the four scenarios. The amount of forest succession (e.g., A2f) was based on the amount cropland and pasture (2010) to forest (2050) in the FORE-SCE change matrices. This transition was simply ignored in the versions of the scenarios that did not allow cropland and pasture to revert to forest.

Each future scenario was implemented separately within SWAT, in addition to NLCD 2001, 2006, and 2011 scenarios. Consistent crop rotations were used in 2001, 2006, 2011, and 2050 scenarios, that is, the same type of corn–soybean rotation variants were implemented on cropland, wherever it occurred, regardless of scenario. Table 1 lists the scenarios that

were run within SWAT. Note that all SWAT behavioral simulations in the 95PPU were run for each land cover scenario, allowing for propagation of parameter uncertainty.

2.4 | Drinking water treatment analysis

Water quality degradation is a concern for most drinking water quality managers because it tends to increase treatment costs (Dearmont et al., 1998; Postel & Thompson, 2005) and may increase risks to human health (Ward et al., 2018). Water quality degradation often arises from loss of natural lands to agricultural and urban uses, which has motivated many jurisdictions to protect the natural lands in their source water watersheds (Postel & Thompson, 2005, p. 100). Where land cover change is still a concern, such as in MHW, examination of temporal trends in drinking water treatment costs can provide useful background information. For example, absence of a temporal trend may indicate that loss of natural land has not occurred or has been inconsequential relative to its effect on drinking water treatment costs. Trends in drinking water treatment costs were examined without matching water quality data because such data were unavailable: water quality calibration data for SWAT were available from 2001 to 2012, while the MWTDS data were available from 2008 to 2017.

We used AR modeling to examine the time series of treatment chemical application rates. MWTDS provided monthly treatment chemical application rates for 2008–2017, including raw water volume processed, aluminum sulfate (alum), PAC, lime, and CO_2. Alum is used as a coagulant to remove unwanted color and turbidity. PAC is used for taste and odor control. Lime is used to soften (and decarbonate) hard water by removing excess calcium and magnesium. The use of lime also brings many other benefits, including removal of natural organic material, bacteria, viruses, and suspended matter. CO_2 is used to adjust pH after softening. Monthly data for alum were completed only for 2011–2017. There were 84 monthly observations for alum and 120 monthly observations for volume of raw water processed, PAC, lime, and CO_2. Volume of raw water processed was measured in mega-gallons (Mgal; 1000,000 gallons) and treatment chemicals were measured as lbs/Mgal.

AR (regression against itself) models account for the serial autocorrelation that is common in temporal data. Such correlation leads to biased standard errors when ordinary least squares (OLS) regression is applied to model trends; AR models correct for serial correlation to produce unbiased estimates (SAS Institute Inc, 2018). The basic AR model (see Nash et al., 2014, p. 155) is:

$$y_t = A_0 + A_1 \times \text{time} + \mu_t, \tag{1a}$$

$$\mu_t = \sum_{t=1}^{k} \rho_i \mu_{t-1} + \varepsilon_t, \tag{1b}$$

$$\varepsilon_t \sim \text{IN}(0, \sigma^2)\,. \tag{1c}$$

The fitted AR Equation (1a), like OLS, includes an intercept (A_0), slope (A_1), and error term μ_t. The model for the error term (1b) estimates the error term's serial correlation (ρ_i) over k lags, with the remaining error (1c) having a mean of 0 and a variance σ^2. AR models were implemented with backward selection of between 12 and 18 lags. A minimum of 12 lags was used because we assumed the treatment application rate for a given month was correlated with the application rate for the same month of the previous year. In some cases, 18 lags were needed to include all possible lags with significant correlation and to obtain the correct statistical test of the significance of model parameters. The backward selection procedure removed lags that were not significant. The AR models were inspected for non-constant error variance (heteroscedasticity) and trend unit roots (SAS Institute Inc, 2018). Neither was found.

Risk management is an inherent aspect of the production of potable water (Crawford-Brown & Crawford-Brown, 2011; Hrudey et al., 2006). To improve potable water quality and minimize risk of contamination, MWTDS shifted the objective of its chemical treatment processes from cost efficiency to water quality (Kraynick, 2020 personal communication). Average before (2008–2014) and after (2015–2017) values (lbs/Mgal) were 206.7 and 290.5 for alum, 71.7 and 91.5 for lime, 1301.5 and 1401.7 for carbon, and 228.7 and 299.6 for CO_2. We included a dummy variable (before = 0; after = 1) in the AR models (Jebb et ah, 2015) to help to disentangle influences of management from trends in chemical application rates.

3 | RESULTS

3.1 | Land cover change

3.1.1 | 2001–2011—A total of 3.5% of the MHW experienced land cover change from 2001 to 2011 (Table A6). This excludes transitions between similar classes (e.g., deciduous forest to evergreen forest or developed low density to developed high density). Most land cover classes experienced both growth and decline. The greatest net gains were by developed land (200 km^2) and grassland (183 km^2), while the greatest net losses were pasture (295 km^2) and forest (266 km^2).

Developed land was unique in experiencing no losses. Urbanization primarily displaced cropland and pasture (and to a lesser extent, forest and wetlands) due to growth in the Minneapolis/St. Paul and St. Cloud metropolitan areas. Cropland expansion occurred, although most is attributable to transition from pasture (234 km^2 of 290 km^2 gross expansion). This transition mostly occurred in the North and South Fork Crow River watersheds (southwest MHW). Cropland also displaced 44 km^2 of wetlands. Most forest loss was converted to shrubland and grassland.

3.1.2 | 2011–2050—Land cover change was projected to be greatest in the A scenarios (Figure 2). Projected land cover changes for A2 and A2f scenarios were 4.5%–4.7% of the total watershed area and 5.3%–5.5% for the A1B and A1Bf scenarios. The A scenarios projected a net loss of over 1000 km^2 of forest to cropland, pasture, and urban (developed). Wetland loss to cropland and pasture also occurred. The greatest gain was attributed to urban development (replacing cropland and pasture), further expanding the footprint of major metropolitan areas. This amounts to a loss of about 9% of the total forest in the A scenarios, covering 2.7% of the MHW. With the addition of forest regrowth in the f scenarios, forest loss was mitigated to about 8% of the total forested area (2.4% of the MHW). Urban growth is greater in the A1B scenarios (1.7% of total watershed area) versus A2 (1.1%). Finally, cropland and pasture growth were about 0.5%–1.5% of the total watershed area in the A scenarios. The greatest loss of forests and wetlands was projected in the A1B scenario, about 1860 km^2 (3.7%) of the MHW.

On average, B scenario net forest loss and a net urban gain changes were less than half of their A scenario counterparts. The magnitude of gross land cover changes for the B scenarios was smaller than the NLCD-based 3.5% gross land cover change between 2001 and 2011. Relative to the A scenarios, cropland and pasture loss were a relatively significant component of overall B scenario change, especially in the B1f and B2f (forest regrowth) scenarios that offset much of the forest loss. All four B scenarios projected a loss of cropland, varying from 20 km^2 (B2) to almost 220 km^2 (B2f). About 3% of the existing forest was lost (less than 1% of the total watershed area). Overall, 397 km^2 of forests and wetlands were lost in B1, the smallest area loss of any non-regrowth (f) scenario.

Change patterns were consistent across scenarios. Projected transitions from cropland and pasture to developed land occurred primarily in the southern half of the MHW, which is the location of major metropolitan areas and agricultural regions. This change pattern represents an outward growth of developed lands at the expense of rural agricultural land cover. Conversely, projected forest and wetland loss occurred primarily in the northern half of the watershed. Figures A2 through A4 in the Supporting Information demonstrate the differing change patterns in headwaters versus downstream subbasins.

3.2 | Modeled water quality change

3.2.1 | Water quality change 2001–2011—Land cover change between 2001 and 2011 resulted in increases in sediment and TP loads, with little change in TN load at the MWTDS intake (Figure 3). Changes are presented as seasonal averages, starting with the beginning of the water year (October 1): October–November–December (OND), January–February–March (JFM), April–May–June (AMJ), and July–August–September (JAS). The greatest changes are in AMJ, associated with early growing season agricultural operations. Across all simulations, the change was relatively small: the median (of the 95PPU) seasonal change in sediment was between +1.2% and +2.4%, between −0.4% and +0.4% in TN, and +1% to +2% in TP. Changes were greater in the headwaters, where the transition from forest to agriculture was dominant. For example, at USGS 05227500 (Figure 1), median seasonal changes were +2.3% to +6.7% (sediment), +3.5% to +4.5% (TN), and +4.8% to +6.3% (TP).

3.2.2 | Water quality change 2011–2050—Pollutant loads at the MWTDS intake reflect the watershed-scale changes in land cover and highlight uncertainty across scenarios. The magnitude of sediment, TN, and TP load changes from 2011 to 2050 is seasonal, with the greatest projected changes in AMJ and similar, smaller changes in other seasons (Figure 3). The differences in AMJ versus other seasons coincide with the early growing season and highlight the influence of agriculture on water quality at the MWTDS. AMJ experiences declines in sediment load, where the decline is greatest among the forest regrowth scenarios. TN load increases are projected at the intake, except in the B1f and B2f scenarios, where cropland is replaced by forest regrowth and urbanization. TP load in AMJ varies by scenario (increase in A, decrease in B).

There is uncertainty in the direction of change (increase/decrease) across the suite of land cover change scenarios. The A scenarios project increases in TN and TP loads, while the B scenarios project decreases (Figure 3). With the inclusion of forest regrowth, A scenario changes in nutrient loads are moderated, while declines in sediment load are amplified. The B1f and B2f scenarios are the only scenarios that result in decreases in sediment, TN, and TP at the intake.

3.2.3 | Upstream to downstream change (St. Cloud vs. Minneapolis intakes) —Land cover change produced similar changes in sediment, TN, and TP loads at the St. Cloud drinking water intake (near USGS gage 05270700, Figure 1) and the MWTDS (Figure 4). From 2001 to 2011, median changes in seasonal sediment, TN, and TP loads were small: +1.1% to +2.7%, +0.3% to +1.2%, and +1.8% to +2.4%, respectively. From 2011 to 2050, projected change was greatest in AMJ, like MWTDS. Differences between scenarios are also similar at the two intakes: the greatest increases in TN and TP loads were projected to occur in response to land cover change magnitudes and patterns in A1B and A2, with smaller increases (B1 and B2) or declines in loads (B1f, B2f) in B scenarios.

Despite the overall similarity in St. Cloud and Minneapolis sediment, TN, TP 2011–2050 changes, there were notable differences. The magnitudes of change were more extreme at Minneapolis, either much higher or much lower depending on constituent (sediment, TN, TP) and scenario (note difference in *y*-axis scale ranges between Figures 3 and 4). More specifically, the magnitudes and pattern of sediment and TP change tended to be quite different between the two sites, whereas the magnitudes and pattern of TN change tended to be similar. For the A1B scenario, for example, the 2011–2050 projected land cover changes produced a median increase in sediment of 1250 Mg at St. Cloud and a median decline of a 2500 Mg at Minneapolis. These results reflect the influence of the overall pattern of forest-to-cropland change occurring predominantly upstream of St. Cloud, and the results also suggest the Mississippi River corridor between St. Cloud and Minneapolis may be acting as a sediment “trap.” The pattern also suggests the extant natural vegetation in the St. Cloud—Minneapolis corridor is an important component of the “trap,” especially during high-flow events. Changes in sediment, TN, and TP across change scenarios at all other calibration locations are presented in Figures A9 through A16 of the Supporting Information.

3.3 | Drinking water treatment trends

The temporal trend was significant for alum, lime, and carbon (Table 2; Figure 5). Management was not significant. Increases in alum, lime, and carbon attributable to management had no effect on the trend. These results suggest that declining source water quality required higher application rates to produce potable water and that the increased application rates would have been needed regardless of the shift in management philosophy. The converse was true for CO_2; the temporal trend was not significant, but the management variable was strongly significant. Model results suggest that the trend was solely attributable to the change in management philosophy for CO_2 (Figure A5). The trend in the volume of water processed appeared to decline slightly over time, but the temporal trend was not statistically significant (Figure A6).

4 | DISCUSSION

4.1 | Land cover change

The land cover change scenarios present eight possible snapshots of spatially explicit future land cover change. Spatial arrangement and magnitude of land cover change differed across scenarios. The primary spatial trends were as follows: (1) replacement of cropland by developed lands in the southern half of the watershed and (2) replacement of forest by cropland and pasture in the headwaters. The locations of the change, and the magnitude of the change projected to occur in those locations, were driving factors in both scenario differences in sediment, TN, and TP loads, and how those differences manifested spatially in the headwater rivers versus the MWTDS intake.

Land change models are inherently uncertain. Inter-model comparisons demonstrate large uncertainty in change projections to 2050 for the U.S., both in magnitude and pattern of change (Sohl et al., 2016). Scenario uncertainty within an individual model is smaller than variability across models (Sohl et al., 2016). Therefore, the introduction of more land change models into the watershed modeling process would introduce further uncertainty into projections of water quality change, beyond the scenario uncertainty.

Finally, these projections are steady-state when implemented within SWAT. That is, they are constant across a time slice, rather than dynamic, annually changing land cover. This allows for isolating land cover change without introducing the confounding effects of variable weather.

4.2 | Water quality change

The signal of sediment, TN, and TP load changes at the MWTDS intake varies by scenario. This variability is representative of the differences in the underlying scenarios' spatially explicit differences in land cover change. There are three important factors: the magnitude of change, the class-by-class change, and how magnitude and class-by-class change are realized in a spatially explicit Land Use Land Cover (LULC) map. These factors, and how they influence water quality, are apparent in differences among future scenarios and in comparing NLCD 2001, 2006, and 2011 land cover maps.

The location and type of change is particularly important when examining projections in constituent loads in the MHW headwaters versus the MWTDS intake. There are two primary types of change projected by the SRES scenarios: (1) agricultural land loss to developed land that occurs in the southern half of the watershed and (2) forest loss to cropland or pasture in the headwaters. Loss of agricultural land to urban development in the subbasins closest to the MWTDS intake results in projections of decreased sediment loads (and associated phosphorus). Cropland losses result in associated declines in erosion and land application of fertilizers. In the headwaters, forest loss to cropland and pasture (Figures A2 and A3) results in an increase in sediment and nutrient loads (Figure A9). This varies with scenario; the B scenarios and all scenarios that allow for reforestation result in negligible sediment increases or sediment declines in headwater locations, related to the low magnitude of change and potential for cropland and pasture transition back to forest. The contrasting modes of land cover change, summarized by cropland losses to urbanization in the lower half of the watershed and cropland gains at the expense of forests compete for influence on sediment, TN, and TP loads at the MWTDS intake. The prevalence of lakes and wetlands in the northern half of MHW act as a buffer via retention of sediment and associated nutrients, likely protecting the MWTDS intake from some negative impacts of forest lost to cropland.

Seasonality was found to be important. Changes in water quality loads at the MWTDS were greatest in AMJ, coinciding with agricultural operations such as tilling, planting, and fertilizer application. One-third of the watershed's annual precipitation falls during AMJ, coupled with agricultural operations and saturated soils from winter precipitation and snowmelt, results in more runoff-associated sediment and nutrient transport than other seasons.

We can conclude (qualitatively) that the combined uncertainty of the watershed model and the LULC model is greater than the individual uncertainty of either model. As reflected in constituent loads at the MWTDS, the variability in A and B scenarios (and their forest regrowth counterparts) has the most influence. This is because the difference in these projections as reflected in water quality changes results in a change of direction of trend. For example, TN and TP are projected to increase in 2050 in all A scenarios but decline in the B1f and B2f scenarios.

These projections are not a complete picture of water quality in 2050. Rather, they only represent the potential influence of land cover change on water quality. Climate change will likely play a role in future water quality of the MHW. The Upper Midwest U.S. is projected to experience winter and spring precipitation increases, a decrease in proportion of winter precipitation falling as snow, and an increase in the frequency and intensity of heavy precipitation events (Hayhoe et al., 2018). These changes to the seasonality of precipitation and overall changes to the water balance have the potential to increase the magnitude of sediment erosion and nutrient transport, as well as their timing. As is apparent based on the land cover change and how it is reflected in water quality at the MWTDS intake, climate changes in the winter and spring, coinciding with the beginning of the growing season, will influence water quality.

4.3 | Drinking water treatment impacts

The temporal trends we report in per-unit use of treatment chemicals are consistent with previous empirical studies in other locations (Dearmont et al., 1998; Moore & McCarl, 1987). We found a statistically significant increase in usage of three (alum, lime, and carbon) of the four treatment chemicals between 2008 and 2017 and an urbanizing watershed over a partly overlapping time period (2001–2011). In addition, the MHW has continued to urbanize through 2016 (Homer et al., 2020). Most studies that relate drinking water treatment costs to influent water quality and land cover are implicitly based on a space-for-time assumption (Abildtrup et al., 2013; Fiquepron et al., 2013; Warziniack et al., 2017). Land cover, water quality, and treatment costs are measured across several different source supply watersheds and the covariance between either land cover and treatment costs or water quality and treatment costs is used as an inferential indicator of how treatment costs may trend for a single source supply watershed due to temporal changes in land cover or water quality. It was not feasible to relate land cover change to change in alum usage because it was not possible, and perhaps conceptually inappropriate, to compile land cover change information over very short temporal periods (e.g., monthly). Congruent temporal trends in treatment chemical usage and urbanization are suggestive of an association between land cover change and treatment costs.

Because of the scenario-based nature of our main objective and the data necessary to answer that question, it was also not feasible to examine elasticities—estimation of the magnitude of change of a dependent variable (e.g., cost) arising from a unit change in an independent variable (e.g., turbidity; % forest). Reported elasticities tend to be small (<<1) but also depend on how cost is defined (Price & Heberling, 2018). Cost could be treatment chemical expenses only, all operation and maintenance (O&M) expenses, O&M plus capital expenses, or the price of potable water paid by a household (Abildtrup et al., 2013; Fiquepron et al., 2013). We anticipate that elasticities for this study would have been <<1 if based on all O&M costs simply due to the scale of MWTDS, which operates conventional and ultrafiltration facilities, and somewhat larger if applied to the cost of treatment chemicals only.

Implicit but perhaps less considered in the calculation of elasticities specifically and the relationship between land cover and drinking water treatment more broadly is the value of the land cover–cost relationship to planning. For example, Elias et al. (2014) modeled the effect of forest loss on organic carbon to understand potential difficulties that plausible land cover change could impose on meeting U.S. Environmental Protection Agency (USEPA) phase II disinfection byproduct rule regulations. The long-term land-cover change scenarios were undertaken to aid the planning process. Plausible visions of future (2050) land cover composition and its effect on influent TN, TP, and sediment provide MWTDS with information that can be used to determine whether treatment processes may need to be adjusted in the future.

Elevated nitrogen concentrations in surface waters, a concern in Minnesota (MPCA, 2013), elsewhere in the Midwest (Hanson et al., 2016), and throughout the U.S. (Davidson et al., 2012), is one planning-related issue that MWTDS may face in the future. The SDWA Maximum Contaminant Level (MCL) for nitrate-N (NO_3-N) is 10 mg/L (USEPA).

Emerging literature on a host of potential adverse health effects suggests a lower MCL may promote disease avoidance (Temkin et al., 2019). The MHW is free of nitrate-N concentrations above the established MCL, but long-term trends (since ~1975) have increased 100% or more (MPCA, 2013). Our results for the A1B and A2 scenarios suggest that land cover composition changes would contribute further to increases in nitrate and other forms of N to the water influent at the MWTDS intake. Current methods for removal of nitrate from drinking water are expensive, variable in efficiency, can produce byproducts that require removal, and do not include the conventional and ultrafiltration processes used by MWTDS (Xu et al., 2017). The combination of a reduction in the MCL for nitrate-N and a further increase in N loads over time has the potential to present challenges to the production of potable water in the future for MWTDS. Removal of N from source water is a widespread challenge across U.S. (Dubrovsky & Hamilton, 2010 ; Nolan & Hitt, 2006).

Harmful algal blooms represent a potential future event facing MWTDS and other water treatment distribution systems (Heisler et al., 2008). In lotic systems, they tend to occur in nutrient-rich waters in late summer when temperatures are warm and river volumes are low (Paerl et al., 2018). Agriculture and urban land cover are commonly cited as the sources of nutrient over-enrichment (Heisler et al., 2008; Paerl et al., 2018). Harmful algae blooms occurred at the mouth of the Maumee River in August 2015 (He et al., 2016) and along the Ohio River in 2015 and 2019. Removal of cyanobacteria cells and cyanotoxins, an important distinction, requires adjustments to conventional treatment process (He et al., 2016). A plausible interpretation of results for the A scenarios is that late summer harmful algal blooms are possible in the MWTDS watershed in the future, given the simulated increase in nutrients.

Although not directly addressed in our modeling, projected population growth in the watershed (MN State Demographic Center, 2019b) associated with urbanization brings other threats to the MWTDS that were not explicitly included in this study. As the MHW population grows, contaminants of emerging concern (CECs), such as pharmaceuticals and personal-care products, are more likely to enter the MWTDS source water in greater amounts. Some CECs survive wastewater treatment and are released as effluent discharge into surface and groundwater (Glassmeyer et al., 2017). Growth of population centers and subsequent increases of CECs in MWTDS source water may be a future reality (Fairbairn et al., 2016; James et al., 2016).

4.4 | Applicability of modeling approach to other locations

Soil Water and Assessment Tool is a widely used water quality model Douglas-Mankin et al. (2010). The modeling undertaken here could be applied to a wide variety of locations across the U.S. and elsewhere, although model selection is dependent on the drinking water source. There is an ever-increasing breadth of forecasted land cover data (e.g., Hurt et al., 2020) that can be downscaled, as demonstrated here, to existing land cover data (e.g., https://worldcover2020.esa.int/). The work by Elias et al. (2014) is the only other effort known to the authors that models the effects of forecasted land cover change on source water quality. Water quality degradation due to increased sediment, phosphorus, and nitrogen is a global threat to source water watersheds (McDonald et al., 2016). It is likely that the forecasted

effects of land cover change reported here would inform planning in other source water watersheds.

5 | CONCLUSIONS

Empirical relationships between land cover and influent water quality and their effect on drinking water treatment costs have been prevalent in the recent academic literature. The value of these relationships to planning has received less attention. The results reported herein indicate that the land use changes that take place over the next 30 years will influence the future plans of the MWTDS. Somewhat conversely, the scenario projections also suggest that the MWTDS has a vested stake in the land use decisions made throughout the watershed over the next 30 years to preserve pre-treatment source water quality. Land use change scenario outcomes reflecting sustainability and equity are likely to present fewer management challenges than scenario outcomes reflecting prioritization of economic growth.

Supplementary Material

Refer to Web version on PubMed Central for supplementary material.

ACKNOWLEDGMENTS

The research described in this paper has been funded by the U.S. Environmental Protection Agency. We thank the anonymous reviewers and Matt Heberling (USEPA) for their valuable comments on earlier versions of the paper. The paper has been subjected to Agency review and has been approved for publication. The views expressed in this journal article are those of the authors and do not necessarily reflect the views or policies of the USEPA. Mention of trade names or commercial products does not constitute endorsement or recommendation for use.

DATA AVAILABILITY STATEMENT

Data will be posted on USEPA's Environmental Dataset Gateway (https://edg.epa.gov/EPADataCommons/Public/ORD/EnviroAtlas/UMRB_SourceWater_WaterQuality.zip).

REFERENCES

Abbaspour K. 2007. “User Manual for SWAT-CUP, SWAT Calibration and Uncertainty Analysis Programs.” Swiss Fed. Inst. Aquat. Sci. Technol. Eawag Duebendorf Switz 93. https://swat.tamu.edu/media/114860/usermanual_swatcup.pdf.

Abbaspour KC, Rouholahnejad E, Vaghefi S, Srinivasan R, Yang H, and Kløve B. 2015. “A Continental-Scale Hydrology and Water Quality Model for Europe: Calibration and Uncertainty of a High-Resolution Large-Scale SWAT Model.” Journal of Hydrology 524: 733–52. 10.1016/j.jhydrol.2015.03.027.

Abildtrup J, Garcia S, and Stenger A. 2013. “The Effect of Forest Land Use on the Cost of Drinking Water Supply: A Spatial Econometric Analysis.” Ecological Economics 92: 126–36. 10.1016/j.ecolecon.2013.01.004.

Arnold JG, Kiniry JR, Srinivasan R, Williams JR, Haney EB, and Neitsch SL. 2012. Soil and Water Assessment Tool Input/Output Documentation Version 2012. College Station, TX: Texas Water Resources Institute. TR-439.

Arnold JG, Srinivasan R, Muttiah RS, and Williams JR. 1998. “Large Area Hydrologic Modeling and Assessment Part I: Model Development.” Journal of the American Water Resources Association 34: 73–89. 10.1111/j.1752-1688.1998.tb05961.x.

Bierman PM, Rosen CJ, Venterea RT, and Lamb JA. 2012. “Survey of Nitrogen Fertilizer Use on Corn in Minnesota.” Agricultural Systems 109: 43–52. 10.1016/j.agsy.2012.02.004.

Colby SL, and Ortman JM. 2017. “Projections of the Size and Composition of the US Population: 2014 to 2060: Population Estimates and Projections.” https://www.census.gov/content/dam/Census/library/publications/2015/demo/p25-1143.pdf.

Crawford-Brown D, and Crawford-Brown S. 2011. “The Precautionary Principle in Environmental Regulations for Drinking Water.” Environmental Science & Policy 14: 379–87. 10.1016/j.envsci.2011.02.002.

Davidson EA, David MB, Galloway JN, Goodale CL, Haeuber R, Harrison JA, Howarth RW, et al. . 2012. “Excess Nitrogen in the U.S. Environment: Trends, Risks, and Solutions.” Issues in Ecology 15. https://www.esa.org/wp-content/uploads/2013/03/issuesinecologyl5.pdf.

Dearmont D, McCarl BA, and Tolman DA. 1998. “Costs of Water Treatment Due to Diminished Water Quality: A Case Study in Texas.” Water Resources Research 34: 849–53. 10.1029/98WR00213.

Douglas-Mankin KR, Srinivasan R, and Arnold JG. 2010. “Soil and Water Assessment Tool (SWAT) Model: Current Developments and Applications.” Transactions of the American Society of Agricultural and Biological Engineers 53: 1423–31.

Dubrovsky NM, and Hamilton PA. 2010. Nutrients in the Nation’s Streams and Groundwater: National Findings and Implications. Reston, VA: U.S. Geological Survey Fact Sheet 2010-3078.

Elias E, Laband D, Dougherty M, Lockaby G, Srivastava P, and Rodriguez H. 2014. “The Public Water Supply Protection Value of Forests: A Watershed-Scale Ecosystem Services Analysis Based upon Total Organic Carbon.” Open Journal of Ecology 4: 517–31. 10.4236/oje.2014.49042.

Fairbairn DJ, Karpuzcu ME, Arnold WA, Barber BL, Kaufenberg EF, Koskinen WC, Novak PJ, Rice PJ, and Swackhamer DL. 2016. “Sources and Transport of Contaminants of Emerging Concern: A Two-Year Study of Occurrence and Spatiotemporal Variation in a Mixed Land Use Watershed.” Science of the Total Environment 551–552: 605–13. 10.1016/j.scitotenv.2016.02.056.

Fiquepron J, Garcia S, and Stenger A. 2013. “Land Use Impact on Water Quality: Valuing Forest Services in Terms of the Water Supply Sector.” Journal of Environmental Management 126: 113–21. 10.1016/j.jenvman.2013.04.002. [PubMed: 23681358]

Glassmeyer ST, Furlong ET, Kolpin DW, Batt AL, Benson R, Boone JS, Conerly O, et al. 2017. “Nationwide Reconnaissance of Contaminants of Emerging Concern in Source and Treated Drinking Waters of the United States.” Science of the Total Environment 581–582: 909–22. 10.1016/j.scitotenv.2016.12.004.

Hanson MJ, Keller A, Boland MA, and Lazarus WF. 2016. “The Debate about Farm Nitrates and Drinking Water.” Choices 31: 1–7. https://www.choicesmagazine.org/UserFiles/file/cmsarticle_485.pdf.

Harmel RD, Cooper RJ, Slade RM, Haney RL, and Arnold JG. 2006. “Cumulative Uncertainty in Measured Streamflow and Water Quality Data for Small Watersheds.” Transactions of the American Society of Agricultural and Biological Engineers 49: 689–701. 10.13031/2013.20488.

Hayhoe K, Wuebbles DJ, Easterling DR, Fahey DW, Doherty S, Kossin JP, Sweet WV, Vose RS, and Wehner MF. 2018. “Our Changing Climate.” In Impacts, Risks, and Adaptation in the United States: Fourth National Climate Assessment (Volume II), edited by Wuebbles DJ, 72–144. Washington, DC: U.S. Global Change Research Program. 10.7930/NCA4.2018.CH2.

He X, Liu YL, Conklin A, Westrick J, Weavers LK, Dionysiou DD, Lenhart JJ, Mouser PJ, Szlag D, and Walker HW. 2016. “Toxic Cyanobacteria and Drinking Water: Impacts, Detection, and Treatment.” Harmful Algae, Global Expansion of Harmful Cyanobacterial Blooms: Diversity, Ecology, Causes, and Controls 54: 174–93. 10.1016/j.hal.2016.01.001.

Heberling MT, Nietch CT, Thurston HW, Elovitz M, Birkenhauer KH, Panguluri S, Ramakrishnan B, Heiser E, and Neyer T. 2015. “Comparing Drinking Water Treatment Costs to Source Water Protection Costs Using Time Series Analysis.” Water Resources Research 51: 8741–56. 10.1002/2014WR016422.

Heisler J, Gilbert PM, Burkholder JM, Anderson DM, Cochlan W, Dennison WC, Dortch Q, et al. 2008. “Eutrophication and Harmful Algal Blooms: A Scientific Consensus.” Harmful Algae, HABs and Eutrophication 8: 3–13. 10.1016/j.hal.2008.08.006.

Homer C, Dewitz J, Jin S, Xian G, Costello C, Danielson P, Gass L, et al. 2020. "Conterminous United States Land Cover Change Patterns 2001–2016 from the 2016 National Land Cover Database." ISPRS Journal of Photogrammetry and Remote Sensing 162: 184–99. [PubMed: 35746921]

Homer C, Dewitz J, Yang L, Jin S, Danielson P, Xian G, Coulston J, Herold N, Wickham J, and Megown K. 2015. "Completion of the 2011 National Land Cover Database for the Conterminous United States–Representing a Decade of Land Cover Change Information." Photogrammetric Engineering and Remote Sensing 81: 345–54. 10.14358/PERS.81.5.346.

Hrudey SE, Hrudey EJ, and Pollard SJT. 2006. "Risk Management for Assuring Safe Drinking Water." Environment International 32: 948–57. 10.1016/j.envint.2006.06.004. [PubMed: 16839605]

Hurt GC, Chini L, Sahajpal R, Frolking S, Bodirsky BL, Calvin K, Doelman JC, et al. 2020. "Harmonization of Global Land Use Change and Management for the Period 850–2100 for CMIP6." Geoscientific Model Development 13: 5425–64. 10.5194/gmd-13-5425-2020.

James CA, Miller-Schulze JP, Ultican S, Gipe AD, and Baker JE. 2016. "Evaluating Contaminants of Emerging Concern as Tracers of Wastewater from Septic Systems." Water Research 101: 241–51. 10.1016/j.watres.2016.05.046. [PubMed: 27262552]

Jebb AT, Tay L, Wang W, and Huang Q. 2015. "Time Series Analysis for Psychological Research: Examining and Forecasting Change." Frontiers in Psychology 6: 727. 10.3389/fpsyg.2015.00727. [PubMed: 26106341]

Lark TJ, Larson B, Schelly I, Batish S, and Gibbs HK. 2019. "Accelerated Conversion of Native Prairie to Cropland in Minnesota." Environmental Conservation 46: 155–62. 10.1017/S0376892918000437.

Lark TJ, Meghan Salmon J, and Gibbs HK. 2015. "Cropland Expansion Outpaces Agricultural and Biofuel Policies in the United States." Environmental Research Letters 10: 044003. 10.1088/1748-9326/10/4/044003.

Martinuzzi S, Radeloff VC, Joppa LN, Hamilton CM, Helmers DP, Plantinga AJ, and Lewis DJ. 2015. "Scenarios of Future Land Use Change around United States' Protected Areas." Biological Conservation 184: 446–55. 10.1016/j.biocon.2015.02.015.

McDonald RI, Weber KF, Padowski J, Boucher T, and Shemie D. 2016. "Estimating Watershed Degradation over the Last Century and its Impact on Water-Treatment Costs for the world's Large Cities." Proceedings of the National Academy of Sciences of the United States of America 113: 9117–22. 10.1073/pnas.1605354113. [PubMed: 27457941]

Mladenoff DJ, Sahajpal R, Johnson CP, and Rothstein DE. 2016. "Recent Land Use Change to Agriculture in the U.S. Lake States: Impacts on Cellulosic Biomass Potential and Natural Lands." PLoS One 11. 10.1371/journal.pone.0148566.

MN State Demographic Center. 2019a. "Population Data." MN State Demogr. Cent. Our Estim https://mn.gov/admin/demography/data-by-topic/population-data/our-estimates/.

MN State Demographic Center. 2019b. "Population Projections." MN State Demogr. Cent. Popul. Proj https://mn.gov/admin/demography/data-by-topic/population-data/our-projections/.

Moore WB, and McCarl BA. 1987. "Off-Site Costs of Soil Erosion: A Case Study in the Willamette Valley." Western Journal of Agricultural Economics 12: 42–49. https://ideas.repec.org/a/ags/wjagec/32477.html.

Moriasi DN, Arnold JG, Van Liew MW, Bingner RL, Harmel RD, and Veith TL. 2007. "Model Evaluation Guidelines for Systematic Quantification of Accuracy in Watershed Simulations." Transactions of the American Society of Agricultural and Biological Engineers 50: 885–900.

MPCA. 2013. Nitrogen in Minnesota Surface Waters: Conditions, Trends, Sources, and Reduction (No. Wq-s6-26a). St. Paul, MN: Minnesota Pollution Control Agency, https://www.pca.state.mn.us/sites/default/files/wq-s6-26a.pdf.

Nakicenovic N, Alcamo J, Davis G, Vries BD, Fenhann J, Gaffin S, Gregory K, et al. 2000. Special Report on Emissions Scenarios (SRES), a Special Report of Working Group III of the Intergovernmental Panel on Climate Change. Cambridge, UK: Cambridge University Press.

Nash MS, Bradford DF, Wickham JD, and Wade TG. 2014. "Detecting Change in Landscape Greenness over Large Areas: An Example for New Mexico, USA." Remote Sensing of Environment 150: 152–62. 10.1016/j.rse.2014.04.023.

Neitsch SL, Arnold JG, Kiniry JR, and Williams JR. 2011. Soil and Water Assessment Tool Theoretical Documentation Version 2009 (No. TR-406). College Station, TX: Texas Water Resources Institute, https://swat.tamu.edu/media/99192/swat2009-theory.pdf.

Nolan BT, and Hitt KJ. 2006. "Vulnerability of Shallow Groundwater and Drinking-Water Wells to Nitrate in the United States." Environmental Science & Technology 40: 7834–40. 10.1021/es060911u. [PubMed: 17256535]

Paerl HW, Otten TG, and Kudela R. 2018. "Mitigating the Expansion of Harmful Algal Blooms across the Freshwater-to-Marine Continuum." Environmental Science & Technology 52: 5519–29. 10.1021/acs.est.7b05950. [PubMed: 29656639]

Postel SL, and Thompson BH. 2005. "Watershed Protection: Capturing the Benefits of nature's Water Supply Services." Natural Resources Forum 29: 98–108. 10.1111/j.1477-8947.2005.00119.x.

Price JI, and Heberling MT. 2018. "The Effects of Source Water Quality on Drinking Water Treatment Costs: A Review and Synthesis of Empirical Literature." Ecological Economics 151: 195–209. 10.1016/j.ecolecon.2018.04.014. [PubMed: 30008516]

Runkel RL, Crawford CG, and Cohn TA. 2004. "Load Estimator (LOADEST): A FORTRAN Program for Estimating Constituent Loads in Streams and Rivers (No. 2328–7055)." 10.3133/tm4A5; https://pubs.er.usgs.gov/publication/tm4A5.

SAS Institute Inc. 2018. SAS/STAT® 15.1 User's Guide. Cary, NC: SAS Institute Inc. https://support.sas.com/documentation/onlinedoc/stat/indexchapter.html.

Sleeter BM, Sohl TL, Bouchard MA, Reker RR, Soulard CE, Acevedo W, Griffith GE, et al. 2012. "Scenarios of Land Use and Land Cover Change in the Conterminous United States: Utilizing the Special Report on Emission Scenarios at Ecoregional Scales." Global Environmental Change 22: 896–914. 10.1016/j.gloenvcha.2012.03.008.

Sohl TL, Sayler KL, Bouchard MA, Reker RR, Friesz AM, Bennett SL, Sleeter BM, et al. 2014. "Spatially Explicit Modeling of 1992–2100 Land Cover and Forest Stand Age for the Conterminous United States." Ecological Applications 24:1015–36. 10.1890/13-1245.1. [PubMed: 25154094]

Sohl TL, Sayler KL, Drummond MA, and Loveland TR. 2007. "The FORE-SCE Model: A Practical Approach for Projecting Land Cover Change Using Scenario-Based Modeling." Journal of Land Use Science 2: 103–26. 10.1080/17474230701218202.

Sohl TL, Wimberly MC, Radeloff VC, Theobald DM, and Sleeter BM. 2016. "Divergent Projections of Future Land Use in the United States Arising from Different Models and Scenarios." Ecological Modelling 337: 281–97. 10.1016/j.ecolmodel.2016.07.016.

Strengers B, Leemans R, Eickhout B, de Vries B, and Bouwman L. 2004. "The Land-use Projections and Resulting Emissions in the IPCC SRES Scenarios Scenarios as Simulated by the IMAGE 2.2 Model." GeoJournal 61: 381–393. 10.1007/s10708-004-5054-8.

Temkin A, Evans S, Manidis T, Campbell C, and Naidenko OV. 2019. "Exposure-Based Assessment and Economic Valuation of Adverse Birth Outcomes and Cancer Risk Due to Nitrate in United States Drinking Water." Environmental Research 176: 108442. 10.1016/j.envres.2019.04.009. [PubMed: 31196558]

Tiemann M. 2017. Safe Drinking Water Act (SDWA): A Summary of the Act and its Major Requirements. Washington, DC: Congressional Research Service. https://www.everycrsreport.com/reports/RL31243.html.

USDA. 2010. Field Crops: Usual Planting and Harvesting Dates (No. Agricultural Handbook Number 628). United States Department of Agriculture, National Agricultural Statistics Service. https://www.nass.usda.gov/Publications/Todays_Reports/reports/fcdate10.pdf.

van Vuuren DP, Lucas PL, and Hilderink H. 2007. "Downscaling Drivers of Global Environmental Change: Enabling Use of Global SRES Scenarios at the National and Grid Levels." Global Environmental Change 17: 114–30. 10.1016/j.gloenvcha.2006.04.004.

van Vuuren DP, Smith SJ, and Riahi K. 2010. "Downscaling Socioeconomic and Emissions Scenarios for Global Environmental Change Research: A Review." WIREs Climate Change 1: 393–404. 10.1002/wcc.50.

Ward M, Jones R, Brender J, de Kok T, Weyer P, Nolan B, Villanueva C, and van Breda S. 2018. "Drinking Water Nitrate and Human Health: An Updated Review." International Journal

of Environmental Research and Public Health 15:1557. 10.3390/ijerph15071557. [PubMed: 30041450]

Warziniack T, Sham CH, Morgan R, and Feferholtz Y. 2017. "Effect of Forest Cover on Water Treatment Costs." Water Economics and Policy 3: 1750006. 10.1142/S2382624X17500060.

Weidner E, and Todd A. 2011. From the Forest to the Faucet: Drinking Water and Forests in the US. Washington, DC: Methods Papaper. USDA Forest Service. https://www.fs.fed.us/ecosystemservices/pdf/forests2faucets/F2F_Methods_Final.pdf.

Wickham JD,Wade TG, and Riitters KH. 2011. "An Environmental Assessment of United States Drinking Water Watersheds." Landscape Ecology 26: 605–16. 10.1007/s10980-011-9591-5.

Xu J, Pu Y, Qi WK, Yang XJ, Tang Y, Wan P, and Fisher A. 2017. "Chemical Removal of Nitrate from Water by Aluminum-Iron Alloys." Chemosphere 166: 197–202. 10.1016/j.chemosphere.2016.09.102. [PubMed: 27697708]

Research Impact Statement

Future urbanization and cropland expansion in the Mississippi headwaters watershed may present planning challenges for potable water production in Minneapolis due to projected N and P increases.

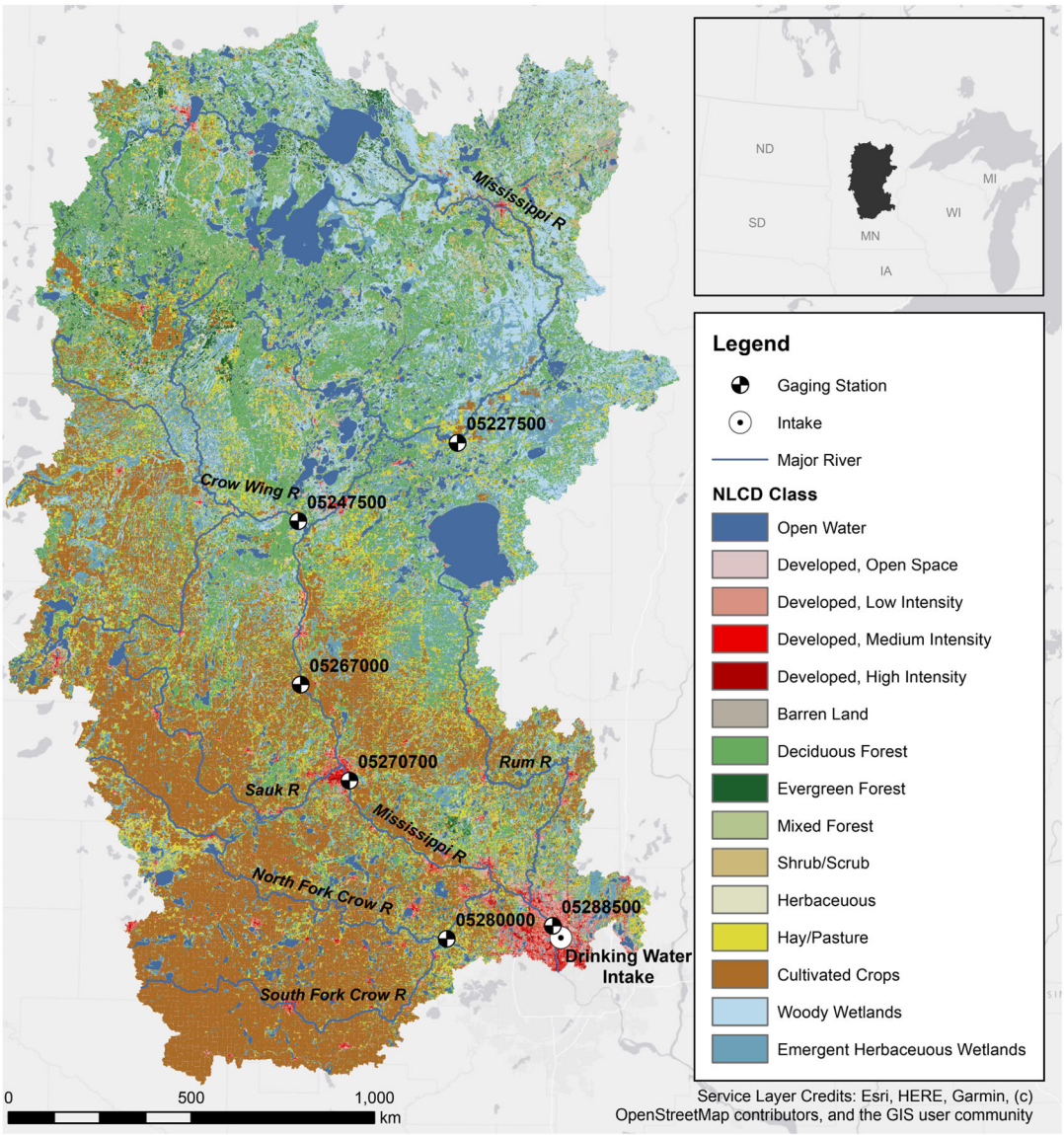

FIGURE 1.

Mississippi Headwaters Watershed (MHW) study watershed (hydrologic unit code 0701), National Land Cover Database (NLCD) 2011 (Homer et al., 2015), United States Geological Survey (USGS) gaging stations used in Soil Water and Assessment Tool (SWAT) calibration, and the Minneapolis Water Treatment Distribution Service (MWTDS) drinking water intake (approximately co-located with USGS gage 05288500).

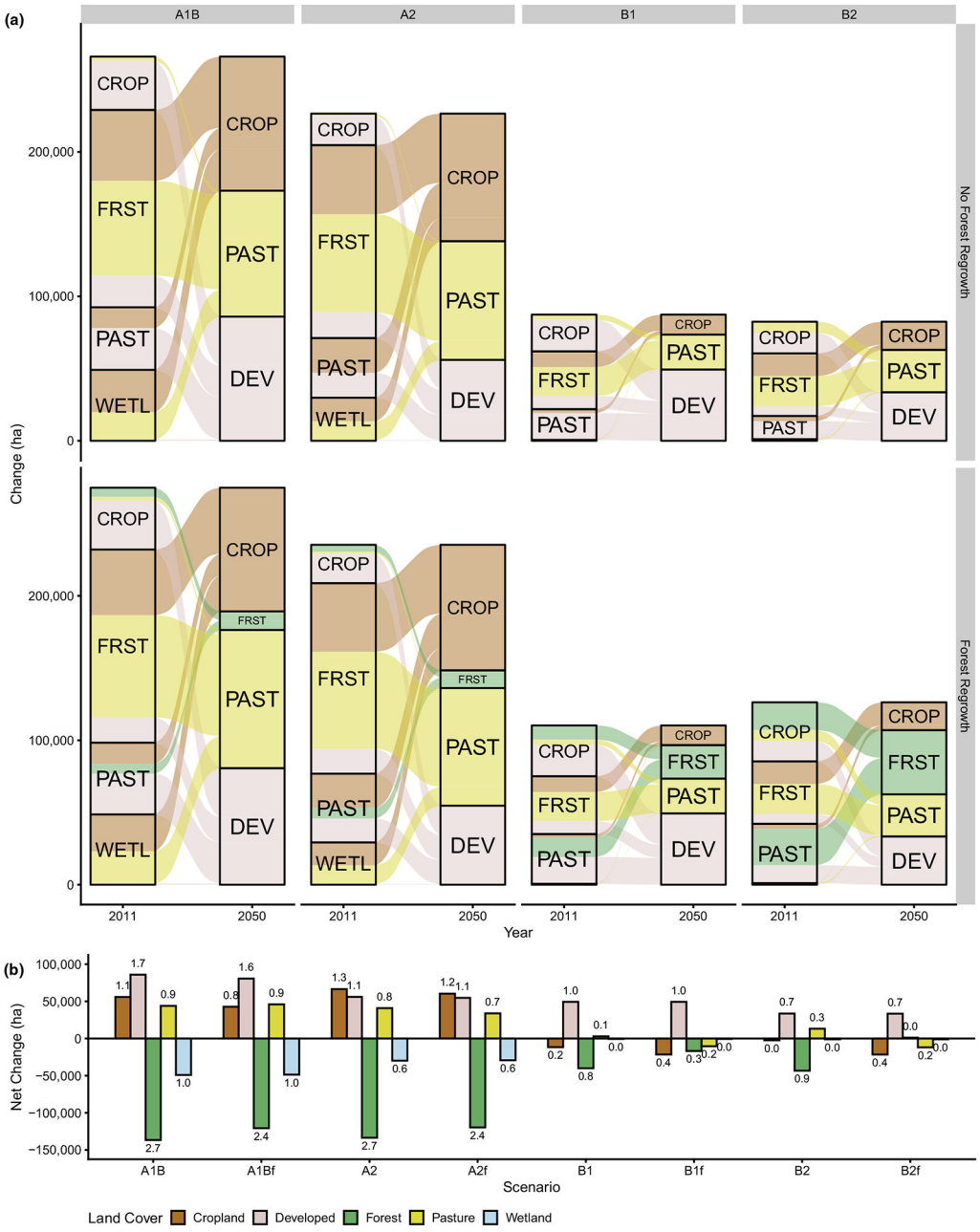

FIGURE 2.

(a) Inter-class land cover changes from 2011 to 2050 by scenario, where colors represent the new land cover class in 2050. (b) Net land cover changes by scenario. CROP, cropland; DEV, developed; FRST, forest; PAST, pasture; WETL, wetland. Labels above bars in panel b represent percentage of total watershed area that changed.

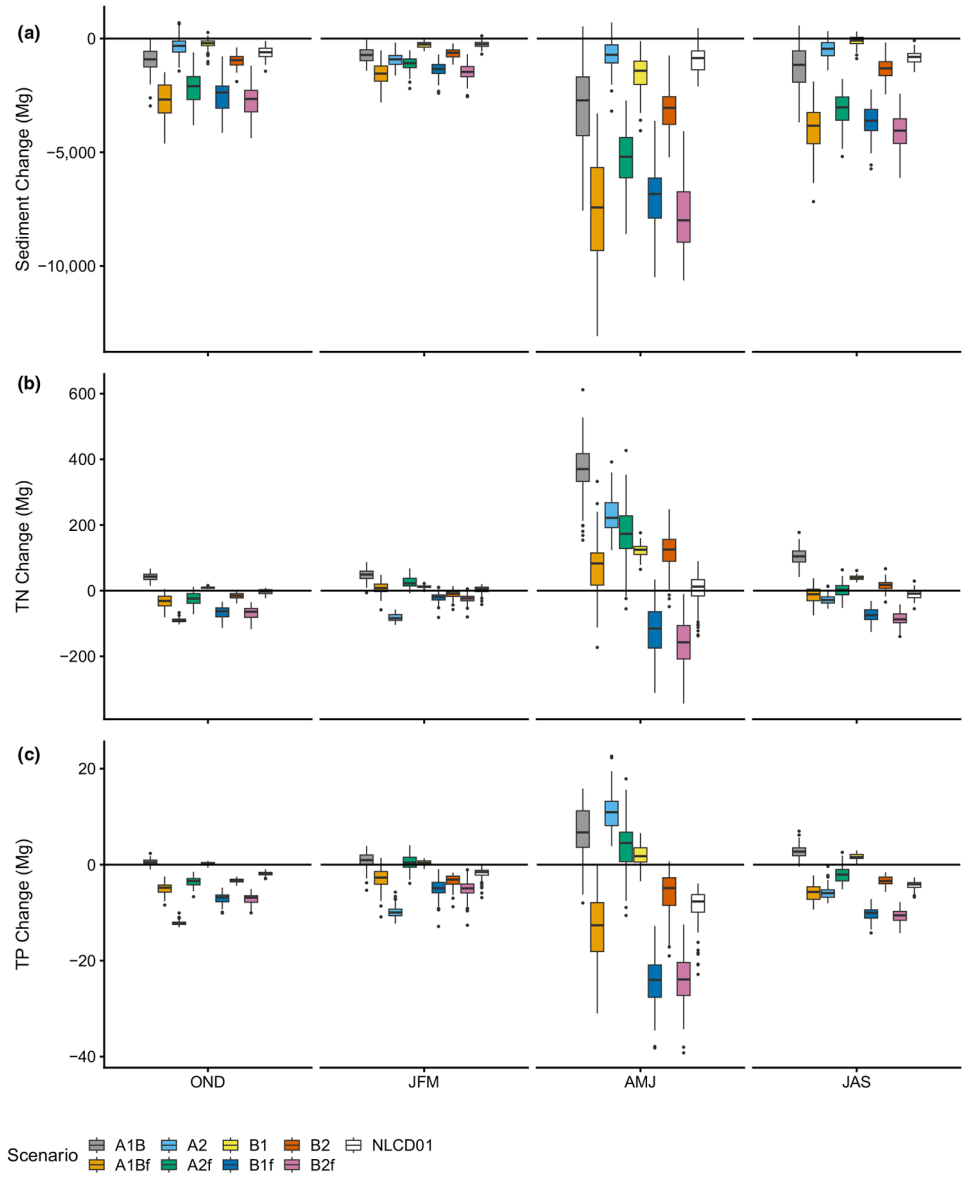

FIGURE 3.

Average seasonal loading differences between NLCD 2011 (modeled) and 2050 scenarios (plus NLCD 2001) at the MWTDS intake for sediment (a), total nitrogen (TN) (b), and total phosphorus (TP) (c). AMJ, April–May–June; JAS, July–August–September; JFM, January–February–March; OND, October–November–December. Boxplots represent model uncertainty constructed from $n = 74$ behavioral simulations that represent the 95PPU parameter uncertainty from SWAT. Boxplots represent median, first and third quartiles (lower and upper hinge, respectively), and values within 1.5 × interquartile range are represented by whiskers. Dots represent outlying values beyond the 1.5 × interquartile range.

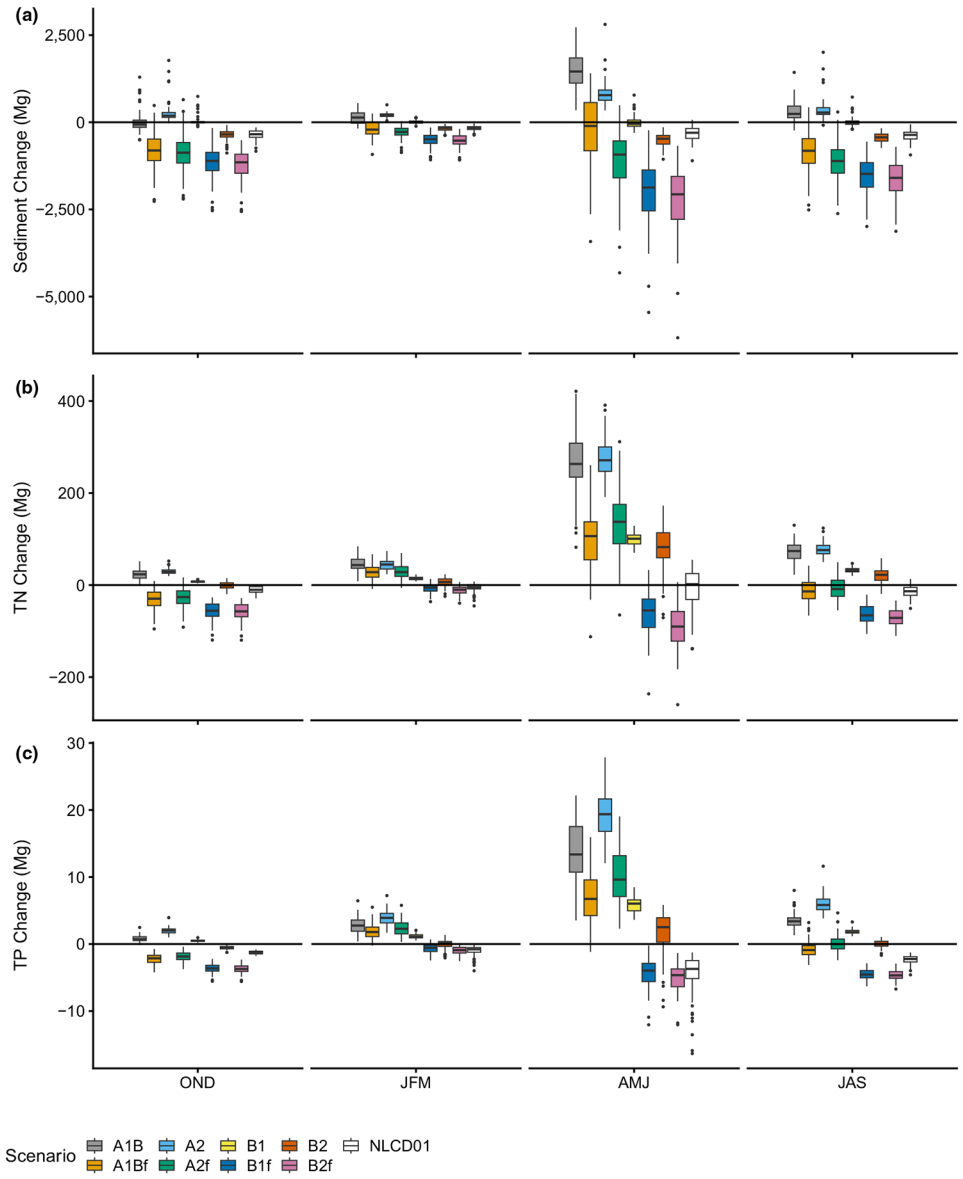

FIGURE 4.

Average seasonal loading differences between NLCD 2011 (modeled) and 2050 scenarios (plus NLCD 2001) near the St.Cloud drinking water intake, USGS 05270700, for sediment (a), TN (b), and TP (c). AMJ, April–May–June; JAS, July–August–September; JFM, January–February–March; OND, October–November–December. Boxplots represent model uncertainty, constructed from $n = 74$ behavioral simulations that represent the 95PPU parameter uncertainty from SWAT. Boxplots represent median, first and third quartiles (lower and upper hinge, respectively), and values within 1.5 × interquartile range are represented by whiskers. Dots represent outlying values beyond the 1.5 × interquartile range.

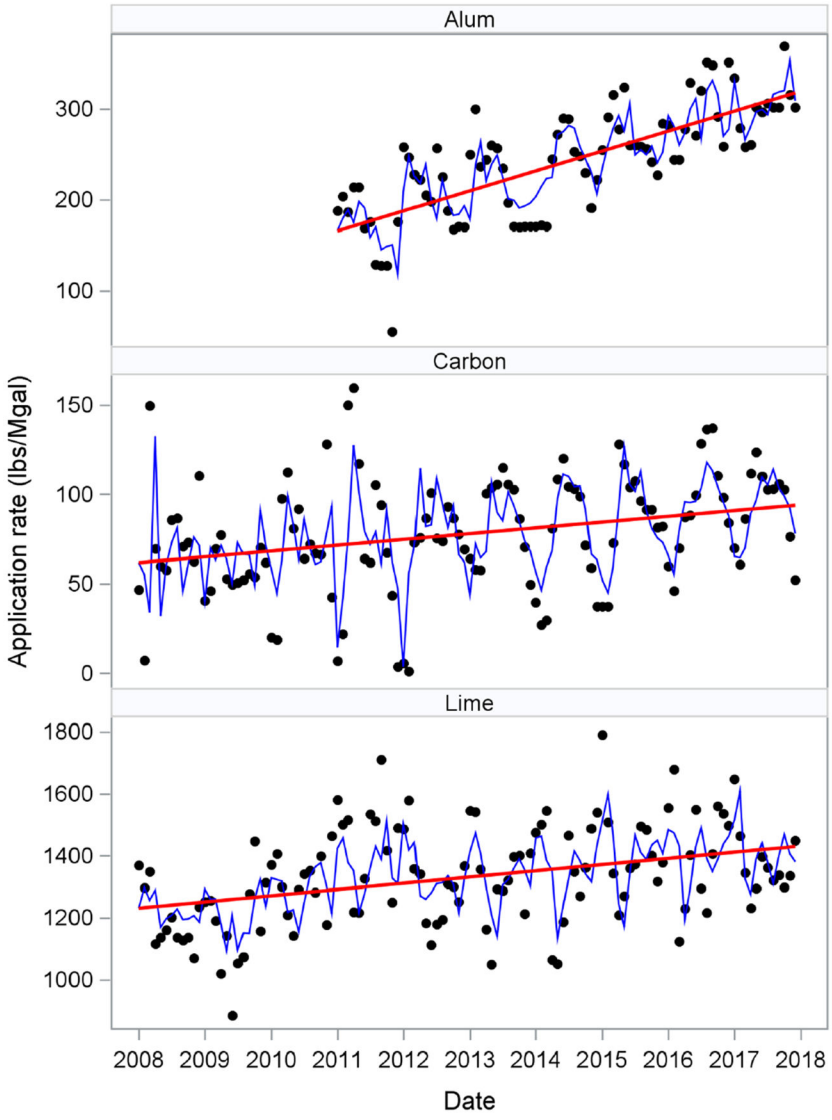

FIGURE 5.

Monthly trends for alum, carbon, and lime (observed (•); modeled (blue line); trend (red line). Slope estimate based on Julian dates (1 = 2008-01-01). Trend slope was significant ($p < 0.05$) for all. Monthly data for alum were incomplete before 2011.

TABLE 1

Land cover scenarios implemented in SWAT, and descriptions of their change characteristics in the MHW.

Year	Land cover	Scenario	Description
2001	NLCD	Baseline	Land cover circa 2001
2006	NLCD	Baseline	Land cover circa 2006
2011	NLCD	Baseline	Land cover circa 2011; used to compare with 2050 scenarios
2050	FORE-SCE	A1B	Forest and wetland losses; developed gain equal to combined cropland and pasture gains. No forest regrowth
2050	FORE-SCE	AlBf	Forest and wetland losses; developed gain equal to combined cropland and pasture gains. Forest regrowth
2050	FORE-SCE	A2	Forest and wetland losses; cropland and pasture gain exceed developed gain. No forest regrowth
2050	FORE-SCE	A2f	Forest and wetland losses; cropland and pasture gain exceed developed gain. Forest regrowth
2050	FORE-SCE	B1	Relatively minor forest and cropland losses; developed gain. No forest regrowth
2050	FORE-SCE	Bit	Relatively minor forest and cropland losses; developed gain. Forest regrowth
2050	FORE-SCE	B2	Relatively minor forest loss; minor developed and pasture gains. No forest regrowth
2050	FORE-SCE	B2f	Cropland and pasture losses. Forest loss and regrowth balanced-little change in total amount of forest

Abbreviation: FORE-SCE, FOREcasting Scenarios of Land-use Change.

TABLE 2

Autoregressive model (A) results and (B) parameters. Significant ($p < 0.05$) parameters are printed in bold typeface. The column tR^2 (total R-square) is the goodness-of-fit for the full model (B), that is, how well the blue line "fits" the black dots in Figure 5.

Treatment	Obs	Intercept	Time	Management	tR^2
(A)					
Alum[a]	84	**−955.5**	**0.0602**		0.73
Lime[a]	120	270.3	**0.0548**		0.48
Carbon[a]	120	−93.4	**0.0088**		0.51
CO_2	120	288.1	−0.0031	**72.04**	0.50
Water[a]	120	**2302.0**	−0.0300		0.79

Alum	Lime	Carbon	CO_2
(B)			
Intercept = −955.0	Intercept = 270.3	Intercept = −93.4	Intercept = 288.1
Time = 0.0602	Time = 0.0548	Time = 0.0088	Management = 72.0
Lag1 = −0.6204	Lag1 = −0.4645	Lag1 = −0.5558	Lag1 = −0.0418
Lag2 =0.2068	Lag12 = −0.2925	Lag2 = 0.2463	
Lag6 = 0.2578	Lag14 = 0.2067	Lag6 = 0.1998	
		Lag10 = 0.2704	
		Lag11 = −0.4106	

[a]Results for single variable models (y = time).